2025 IEEE/SICE International Symposium on System Integration (SII)
January 21-24, 2025, Munich, Germany

Comparison of Characteristics of Cycloidal Gear Reducer of 20 Different Combinations of Metal and Plastic Parts

Hironori Satake[1] and Naoyuki Takesue[1]

***Abstract*— In recent years, the demand for industrial robots has increased and is expected to continue to grow. On the other hand, efforts to reduce the global environmental burden are spreading. This paper aims to develop a lightweight reduction gear for energy-saving robots. To reduce the weight of robots, it is necessary to replace conventional metal materials with new lightweight materials. However, in general, weight reduction tends to reduce the rigidity of the robot, resulting in a decrease in the high-speed and high-precision performance required of robots. The authors have studied the possibility of replacing metal parts with machined CFRP, POM, and 3D printer resin parts , and have examined the adaptability of these parts. In the previous paper, weight, no-load running torque, torque-torsional characteristics, and static torque transfer efficiency were compared for 14 different combinations of metal and resin reduction gears. In this paper, the number of reduction gear combinations is increased to 20, and dynamic torque transfer efficiency is added to the comparison. As a result, the effect of the type of resin applied and its combination on the performance of the reduction gears is clarified, and it is shown that weight reduction can be achieved while minimizing performance degradation by selecting the combination that best suits the application.**

I. Introduction

In recent years, the demand for industrial robots has been increasing year by year and is expected to continue to grow in the future[1]. This is due to a decrease in the working-age population, rising wages in emerging countries, and expansion of quality improvement. Conventional robots were mainly used in the manufacture of automobiles and electronic devices, but as robots themselves have become more sophisticated and less expensive, the cost of introducing them has decreased, and robots are being introduced into a variety of industries, including food, medical, and service[2], [3], [4], [5]. Furthermore, the development of cooperative robots that work side-by-side with humans in the field of industrial robotics is advancing, and the industrial robotics market is expected to expand further.

On the other hand, efforts toward the Sustainable Development Goals (SDGs) and carbon neutrality are spreading worldwide. Therefore, energy saving is also desired in industrial robots[6]. The power consumption of an industrial robot is largely related to the robot's own weight, so weight reduction can contribute to energy conservation. To reduce the weight of robots, it is necessary to replace conventional metal materials with new lightweight materials such as non-metals, composite materials, and resins. However, weight reduction generally reduces rigidity, which tends to lower the high-speed and high-precision performance required of industrial robots.

The authors have been studying the adaptability of resin parts by replacing metal parts with parts made of materials such as machinable CFRP, POM, which is an engineering plastic, and resin materials for FDM 3D printers[7], [8], which have attracted attention in recent years, in order to reduce the weight of robots. The evaluation contents and results using metal and plastic reduction gears were presented for the development of the drive unit, which is greatly related to the power and position control performance of the robot[9], [10]. In the previous paper[10], weight, no-load running torque, torque-torsional angle characteristics, and static torque transfer efficiency were compared for 14 different combinations of metal and plastic gear parts.

In this paper, the number of reduction gear combinations is increased to 20, and dynamic torque transfer efficiency, which is an important evaluation item that indicates reduction gear performance, is added to the comparison. As a result, the influence of the type of resin applied and its combination on the performance of the reduction gears is clarified, and it is shown that weight reduction can be achieved while minimizing performance degradation by selecting a combination suitable for the application.

II. Design and Construction of Reduction Gears

As in the previous papers[9], [10], several types of metal and plastic reduction gear components were fabricated in this study, and the reduction gear was configured with the combinations described below in Section III. The metal and resin parts had almost the same shape and dimensions. Some of the metal and resin parts were machined, and some of the resin parts were 3D-printed. An internal planetary gear with an epitrochoidal tooth profile[11] was used as the reduction gear. This gear is considered structurally rigid because the teeth mesh at multiple contacts, has a smooth curved tooth profile, and can be easily fabricated using a machining center

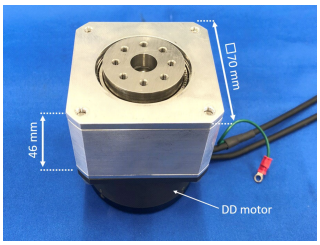

Fig. 1: Exterior of developed metal reduction gear

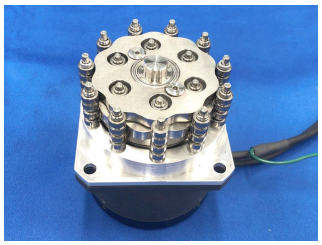

Fig. 2: Interior of developed metal reduction gear

[1]Hironori Satake and Naoyuki Takesue are with Tokyo Metropolitan University, Hino-shi, Tokyo, Japan

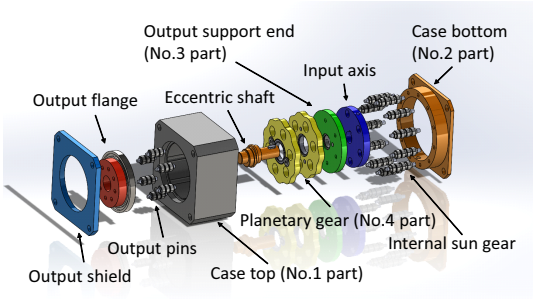

Fig. 3: Exploded view of reduction gear parts

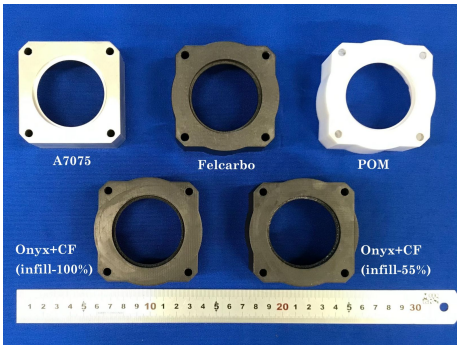

Fig. 4: Case tops made of A7075, Felcarbo, POM, Onyx+CF (infill-100% and 55%)

or 3D printer, and can be made more efficient due to rolling contact.

The same epitrochoid curve and parameters are used with the previous papers[9], [10]. The external and internal structures of the metal reduction gear actually fabricated in the previous paper are shown in Fig. 1 and 2, respectively.

The internal components of the reduction gears are shown in Fig. 3. In this paper, as in the previous paper, two of the four types of parts shown in Table I were fabricated in metal and resin, respectively. The parts made of A7075, SUS304, Felcarbo[12], a machinable carbon fiber reinforced plastic (CFRP) manufactured by Futaba Co., and POM, an engineering plastic were machined. While two types of parts made of Onyx with carbon fiber were fabricated using MarkForged's Mark Two. One of the two types has a 55% infill, which is the maximum fill rate when the cross-sectional structure is triangular, and carbon fibers are inserted into the top and bottom surfaces of the case. The other has a 100% infill, where Onyx is printed across the cross-section without gaps, and carbon fibers are inserted in all layers. The fabricated parts are shown in Fig. 4 and Fig. 5.

Bearings with an outer diameter of $\phi 6.5$ were placed on the internal sun gear and output pins to achieve rolling contact and reduce friction. The internal sun gear was fixed with pin holes (depth 4 mm) in the case top and case bottom, and the output pins were fixed with pin holes (depth 3 mm) in the output flange and output support end. The output flange, output support end and planetary gear were adjusted and maintained with spacers.

III. Evaluation Samples

The four parts shown in Table I, two of which are the Case top and the Planetary gear, are combined with metal and resin, and their driving characteristics is compared. In the previous paper, the combination was only "stiffness of the case top material $\leq$ stiffness of the planetary gear material." In this paper, the combination of "stiffness of the case top material $>$ stiffness of the planetary gear material" is additionally examined to clarify the difference in performance when various materials are applied to the case top and planetary gear. There are 20 combinations of Table II to be evaluated.

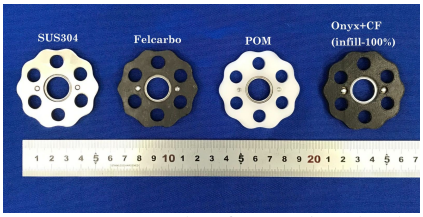

Fig. 5: Planetary gears made of A7075, Felcarbo, POM and Onyx+CF (infill-100%)

TABLE I: Parts and materials

Part number	Parts name	Materials
1	Case top	A7075 Felcarbo POM Onyx+CF (infill-100%) Onyx+CF (infill-55%)
2	Case bottom	A7075
3	Output support end	SUS304
4	Planetary gear	SUS304 Felcarbo POM Onyx+CF (infill-100%)

TABLE II: Combinations

		Planetary gear			
		SUS304	Felcarbo	POM	Onyx+CF (infill-100%)
Case top	A7075	①	⑥	⑪	⑯
	Felcarbo	②	⑦	⑫	⑰
	POM	③	⑧	⑬	⑱
	Onyx+CF (infill-100%)	④	⑨	⑭	⑲
	Onyx+CF (infill-55%)	⑤	⑩	⑮	⑳

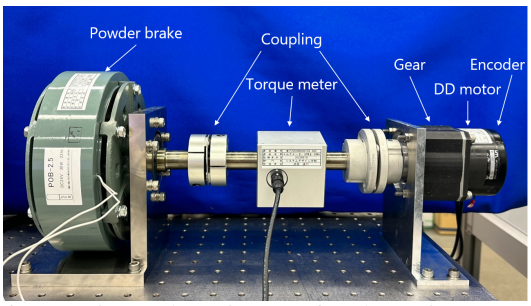

Fig. 6: Experimental equipment for dynamic torque transmission efficiency

IV. Dynamic Torque Transfer Efficiency

In the previous paper[9], [10], static torque transfer efficiency was evaluated by fixing the output shaft side of the

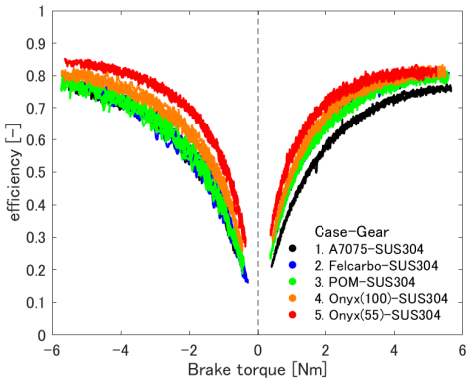

(a) Combination ①–⑤

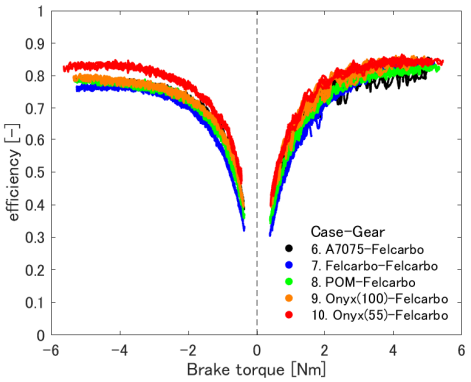

(b) Combination ⑥–⑩

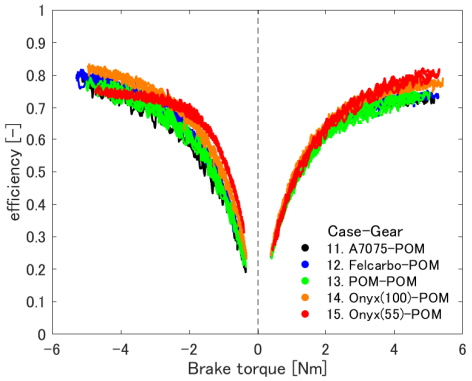

(c) Combination ⑪–⑮

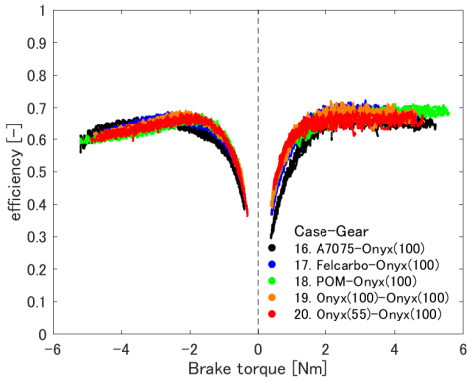

(d) Combination ⑯–⑳

Fig. 7: Dynamic torque transfer efficiency at constant motor speed of ± 100 rpm and varying brake torque

reduction gears. However, the torque transfer efficiency may be changed according to the rotational speed. Therefor, in this paper, the dynamic torque transfer efficiency is measured by rotating the reducer while applying a load by a powder brake. The experimental setup is shown in Fig. 6. A motor (Microtech Laboratory: MDH-7018, instantaneous maximum output 90W) and reduction gear were mounted, the drive side of a torque meter (Unipulse: UTM II-50N·m) was installed on the output shaft, and a powder brake (Sinfonia Technology: POB-2.5) was attached to the load side of the torque meter and fixed to the base.

A. Experimental procedure

Dynamic torque was measured under two conditions, condition 1 and 2, as shown below. In condition 1, the motor command speed was fixed at 100 rpm or -100 rpm, and the load torque by the powder brake was varied at a rate of 0.25 N·m up to 5 N·m, which was measured for three periods. The motor torque τ_{in} is estimated from the torque value τ_{out} measured by the torque meter and the current value of the motor attached to the input side of the reducer. When the reduction ratio is i, the efficiency e is expressed as Eq. (1). This equation is used to calculate the efficiency.

$$e = \frac{\tau_{\mathrm{out}}}{i\tau_{\mathrm{in}}} \tag{1}$$

In condition 2, the command torque of the load torque was fixed at 4.5 N·m and the drive torque was measured for three cycles when the target angular velocity of the motor was varied at a rate of 10 rpm/s to 200 rpm or -200 rpm. As in condition 1, the efficiency e is calculated by Eq. (1).

B. Experimental results

The experimental results for condition 1 are shown in Fig. 7. The vertical axis shows the calculated efficiency and the horizontal axis shows the brake torque on the reducer. Combination ①–⑮ efficiency increases as the brake torque increases. Combination ⑯–⑳, which uses Onyx gear, shows an increase in efficiency up to a load torque of about 2 N·m in the forward and reverse directions, and a decrease in efficiency when the brake torque is above about 2 N·m.

The experimental results for condition 2 are shown in Fig. 8. The vertical axis is the calculated efficiency and the horizontal axis is the angular velocity of the motor corresponding to the input speed of the reducer. For all combinations, the efficiency is nearly constant as the angular velocity changes.

The dynamic torque transfer efficiency at a load torque of 5 N·m and angular velocity of 100 rpm is shown in Fig. 9. Compared to Combination ①, which is composed entirely of metal parts, Combination ②–⑤, in which the case is replaced by resin, is more efficient for combinations with lower case stiffness. The same tendency is observed when the load torque is small or large and when the rotation direction of the reducer is forward or reverse.

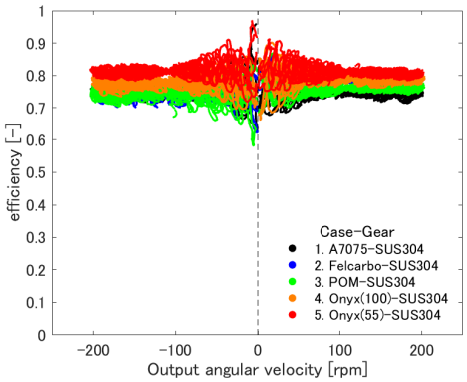

(a) Combination ①–⑤

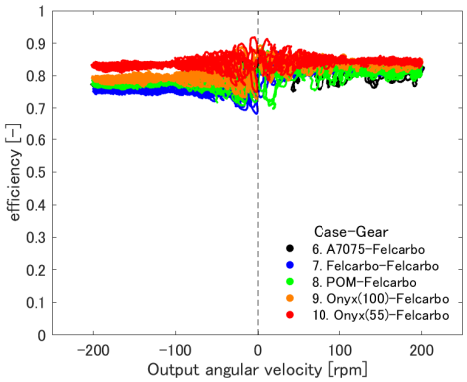

(b) Combination ⑥–⑩

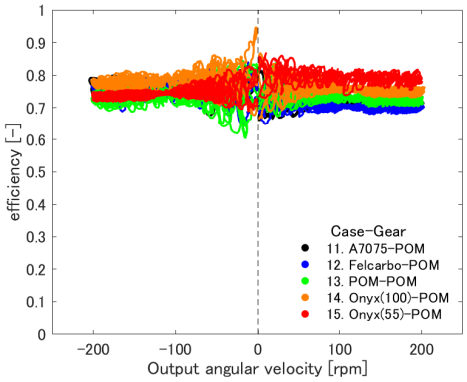

(c) Combination ⑪–⑮

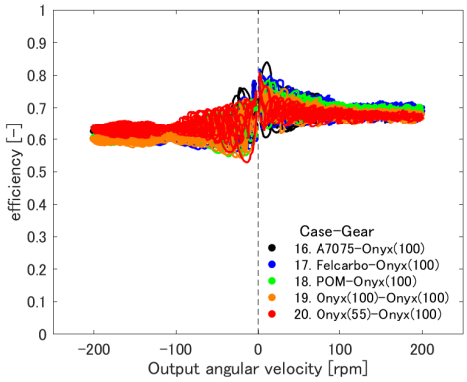

(d) Combination ⑯–⑳

Fig. 8: Dynamic torque transfer efficiency at constant brake torque of 4.5 N·m and varying motor speed

Combination ⑥–⑩ using Felcarbo gears is more efficient when the stiffness of the case top is lower, as is the case with metal gears. In the same case, the efficiency of the combination using Felcarbo is higher than that of the combination using metal gears.

Combination ⑪–⑮ using POM gears shows higher efficiency for combinations with lower case stiffness. However, the results of Condition 1 show that the rate of increase in efficiency decreases when the load torque in the reverse direction of Combination ⑮ is greater than about 2 N·m. Also, using the same case, the efficiency is lower when the gear is POM than when it is metal.

Combination ⑯–⑳ using Onyx gears shows almost no change in efficiency with different case tops, and the efficiency is low.

C. Discussion

When a less rigid material was used for the case top, the efficiency tended to increase. It is considered that the low stiffness of the case top allows for geometric inconsistencies due to fabrication and assembly errors, resulting in a smoother rotation and higher efficiency. When the gear was replaced by Felcarbo, the efficiency tended to be the same or increases, and when the gear was replaced by POM or Onyx, there was a decrease in efficiency. When the gear was Onyx, the stiffness of the case top had little effect on the efficiency. The rigidity of the gear, which is as small as POM or Onyx, is considered to absorb the force applied

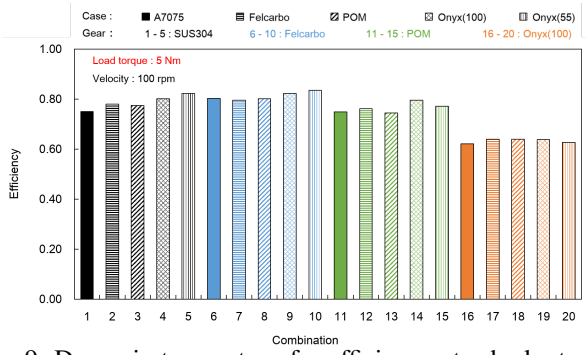

Fig. 9: Dynamic torque transfer efficiency at a brake torque of 5 N·m and angular velocity of 100 rpm

by the motor, resulting in deformation that allows geometric inconsistencies due to fabrication and assembly errors, but does not sufficiently transmit torque to the output shaft of the reducer. When the gears were made of Felcarbo, they were less rigid than metal, but more rigid than POM or Onyx, and the deformation that allowed for geometric inconsistencies in the gears as well as the case enabled smoother rotation than when the gears were metal, and transmitted more torque than when the gears were POM or Onyx. This is considered to be the reason for the increase in efficiency.

V. Other Evaluation Experiments

While the previous paper [10] compared the weight, no-load running torque, and torque–torsional characteristics of

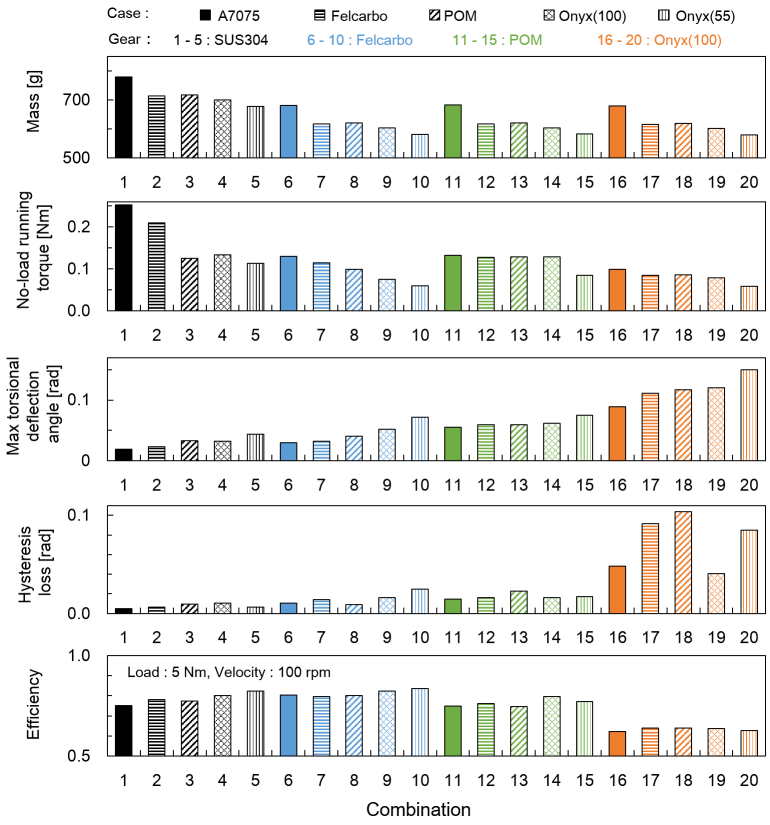

Fig. 10: Summary of characteristics of weight, no-load running torque, maximum torsional angle, hysteresis loss, and dynamic torque transfer efficiency

14 different combinations, this paper presents the comparison of characteristics for 20 different combinations.

A. *Weight evaluation*

The measured weights are shown in the first row of Fig. 10. The density of A7075 is 2.8 g/cm^3, stainless steel is 7.9 g/cm^3, Felcarbo is 1.3 g/cm^3, POM is 1.4 g/cm^3 and Onyx is 1.2 g/cm^3. Combination ①, which uses all metal parts, weighs 779 g. However, Combination ⑳, in which the case is replaced with Onyx(infill-55%)+CF and the gear with Onyx(infill-55%)+CF, weighs 580 g. The weight can be reduced by up to 26% by replacing the metal parts with resin.

B. *No-load running torque*

Next, the no-load running torque was measured. The measurement method is the same as in the previous paper[10]. The motor was mounted on the developed reducer. The drive torque was measured while the target angular velocity of the motor attached to the input side of the reducer is changed at a rate of 10 rpm/s. Since the rated speed of the motor is 200 rpm, the maximum input speed is set to 200 rpm and the motor is driven for three cycles.

The results of the experiment are shown in the second row of Fig. 10. Comparing all the combinations, the values of Combination ① and ② were larger than those of the other combinations. All of these combinations consisted of metal or Felcarbo for the case and SUS304 for the gears. The other combinations reduced the drive torque by 47 to 77%. By using a material with low rigidity for either the case or the gear, it is considered that when torque is applied to the reducer, deformation that allows geometric inconsistencies due to fabrication or assembly errors occurs, resulting in a smooth drive that reduces the drive torque.

C. *Torque-angle characteristics*

Finally, the torque-angle characteristics of the developed gear were evaluated. The measurement method is the same as in the previous paper[10]. A torque meter was installed on the output shaft of the reduction gear and further fixed to the environment. The rated torque of the motor used, 1 N·m, was set as the maximum input torque, and the input torque was varied with a rate of 0.05 N·m/s for three cycles. The torque-torsional angle characteristic of the reducer was obtained from the torque value measured by the torque meter and the angle information of the encoder of the motor attached to the input side of the reducer.

The maximum torsional angle that can be read from the obtained torque-torsional angle characteristics is shown in the third row of Fig. 10. A comparison of all combinations showed that the torsional angle increases with decreasing case stiffness and gear stiffness. The rate of increase in the maximum torsional angle was greater when the gear stiffness was reduced than when the case stiffness was reduced. Therefore, it can be seen that gear stiffness had a greater

effect on the maximum torsional angle than case stiffness. When a material with low stiffness is used for the gear close to the output element, the stiffness has a direct effect on the output angle. However, when a material with low stiffness is used for the case close to the input element, only one-tenth of the reduction ratio affects the output angle, so the effect on the torsional angle is considered small.

The hysteresis loss that can be read from the obtained torque-torsional angle characteristics is shown in the fourth row of Fig. 10. Comparing all combinations, it can be seen that the hysteresis loss was very large when the gear was Onyx(infill-100%)+CF. This indicates that the gear had a greater effect on the hysteresis loss than the case, as does the maximum twist angle. Hysteresis loss is caused by various factors such as backlash, stiffness, and surface roughness. Among the gears used in this study, POM and Onyx(infill-100%)+CF are considered to have similar stiffness, suggesting that machining accuracy has a significant effect on hysteresis loss. In this paper, A7075, Felcarbo, and POM are fabricated by machining, and their accuracy is considered to be similar, but Onyx(infill-100%)+CF is fabricated by a 3D printer and its accuracy is different. The difference may have greatly affected the hysteresis loss.

VI. Conclusion

In this paper, 20 combinations of metal and plastic gear parts were fabricated to investigate the performance, and characteristics such as weight, no-load running torque, torque-torsional characteristics, and efficiency were compared. In particular, the dynamic efficiency of the torque transmission efficiency was measured in detail by rotating the gearbox while applying a load.

Combination ①, consisting entirely of metal parts, had the highest stiffness of all the combinations, but the heaviest weight and the highest no-load running torque. Combination ② had the second highest stiffness after ①, but did not significantly reduce weight or improve efficiency.

The Combination ⑤ and ⑧ to ⑳ has low weight and no-load running torque, but the maximum torsional angle is large and the torque-angle characteristic shows non-linearity , which may limit its suitability for use in robots. In other words, the combination of "stiffness of the material of case top $>$ stiffness of the material of planetary gear," which was not included in the previous paper, is still not suitable as a condition for the reduction gear in this paper. The results of the no-load running torque and torque-torsion characteristics show that the Combination ③, ④, ⑥, and ⑦ have relatively low no-load running torque and torsion angle, and that the combination can reduce weight while minimizing performance degradation among the combinations whose characteristics were evaluated in this study. However, each of these combinations has different characteristics. Therefore, the combinations can be classified by characteristics as follows.

- Weight reduction is important: Combination ⑦
- Efficiency is important: Combinations ④, ⑥, ⑦
- Hysteresis loss is important: Combination ③

The combination of materials should be selected according to which aspect is important for a robot. In the future, it will be necessary to study the characteristics of gear reducers with higher reduction ratios. In addition, the relationship between high-speed rotation, machining accuracy, durability and temperature characteristics is an important issue.

Acknowledgement

This research was subsidized by the New Energy and Industrial Technology Development Organization (NEDO) under project JPNP20016. This paper is an achievement of joint research with and is jointly owned copyrighted material of the ROBOT Industrial Basic Technology Collaborative Innovation Partnership.

We thank Prof. Gen Endo (Tokyo Institute of Technology), Prof. Yusuke Ohta (Chiba Institute of Technology), and Prof. Takeshi Takaki (Hiroshima University) for their valuable comments and discussion.

References

[1] International Federation of Robotics: Global industrial robot sales doubled over the past five years, https://ifr.org/ifr-press-releases/newsglobal-industrial-robot-sales-doubled-over-the-past-five-years, (2022/8/17)

[2] H. Cheng and G. Ji: Design and implementation of a low cost 3D printed humanoid robotic platform, 2016 IEEE International Conference on Cyber Technology in Automation, Control, and Intelligent Systems (CYBER), 2016, pp. 86-91.

[3] Z. Wang, D. S. Chathuranga and S. Hirai: 3D printed soft gripper for automatic lunch box packing, 2016 IEEE International Conference on Robotics and Biomimetics (ROBIO), 2016, pp. 503-508.

[4] Y. Yamanaka, S. Katagiri, H. Nabae, K. Suzumori and G. Endo: Development of a Food Handling Soft Robot Hand Considering a High-speed Pick-and-place Task, 2020 IEEE/SICE International Symposium on System Integration (SII), 2020, pp. 87-92.

[5] Jeong IG, Khandwala YS, Kim JH, et al.: Association of Robotic-Assisted vs Laparoscopic Radical Nephrectomy With Perioperative Outcomes and Health Care Costs, 2003 to 2015. JAMA. 2017;318(16):1561–1568.

[6] K. Nonoyama, Z. Liu, T. Fujiwara, M. Alam,and T. Nishi: Energy-Efficient Robot Configuration and Motion Planning Using Genetic Algorithm and Particle Swarm Optimization, Energies Journal 2022, Volume 15, Issue 6, 2074.

[7] M. Pollák, J. Török, J. Zajac, M. Kočiško and M. Telišková: The structural design of 3D print head and execution of printing via the robotic arm ABB IRB 140, 2018 5th International Conference on Industrial Engineering and Applications (ICIEA), 2018, pp. 194-198.

[8] M. Pollák, J. Kaščak, M. Telišková, J. Tkáč: Design of the 3D Printhead with Extruder for the Implementation of 3D Printing from Plastic and Recycling by Industrial Robot, TEM Journal, Volume 8, Issue 3, pp. 709-713, ISSN 2217-8309.

[9] K. Iizuka, N. Takesue: Comparison of Characteristics of Internal Planetary Gear Reducer with Epitrochoid Curve using Metal and 3D Printed Parts, Proc. The 2023 IEEE/SICE International Symposium on System Integrations (SII 2023), pp.515-520, 2023.

[10] H. Satake, N. Takesue: Comparison of Characteristics of Cycloidal Gear Reducer using Metal, Plastic, and 3D Printed Parts, Proc. The 2024 IEEE/SICE International Symposium on System Integrations (SII 2024), pp.1531-1536, 2024.

[11] T. Yukawa and M. Kaneko: Mechanisms of a cyclo gear reducer with several gear ratios, 2012 Proceedings of SICE Annual Conference (SICE), 2012, pp. 2274-2279.

[12] FUTABA Co., Felcarbo: What is Futaba's CFRP PLATE?, https://www.cfrp.mtb.futaba.co.jp/en/

[13] H. Kanazawa, H. Nabae, K. Suzumori and G. Endo: Mechanical Parts Manufactured by a 3D Printer for Industrial Robot -Part1 : Measuring the accuracy of the hole shape-, Proceedings of the 2021 JSME Conference on Robotics and Mechatronics 2P3-A08.(in Japanese)